

FSU-HEP-930830  
BNL-49462  
August 1993

# THE $t\bar{t}\gamma$ BACKGROUND TO $pp \rightarrow W\gamma + X$ AT THE SSC \*

U. BAUR

*Physics Department  
Florida State University, Tallahassee, FL 32306*

A. STANGE

*Department of Physics,  
Brookhaven National Laboratory, Upton, NY 11973*

## ABSTRACT

We calculate the  $pp \rightarrow t\bar{t}\gamma + X \rightarrow W\gamma + X$  cross section at SSC energies. Approximately 40% of the total cross section originates from photon bremsstrahlung off the final state jet in  $t\bar{t}j$  production. Without cuts restricting the hadronic activity, the  $t\bar{t}\gamma$  rate is a factor 10 (2) larger than the tree level  $W\gamma$  cross section for a top quark mass of 110 GeV (200 GeV). Imposing a jet veto cut, the  $t\bar{t}\gamma$  rate can be suppressed to a level well below the  $W\gamma + 0$  jet signal cross section.

## 1. Introduction

One of the prime targets for experiments at present and future colliders is the measurement of the  $WW\gamma$  and  $WWZ$  couplings. In the Standard Model (SM) of electroweak interactions, these couplings are unambiguously fixed by the non-abelian nature of the  $SU(2) \times U(1)$  gauge symmetry. Experiments at the Tevatron, HERA and LEP II are expected to measure the three vector boson couplings at the 10 – 20% level at best [1, 2]. High precision tests have to await the SSC or LHC [2, 3, 4].

A suitable process to study the  $WW\gamma$  vertex at the SSC is  $W^\pm\gamma$  production [2, 3]. Present studies indicate that the background from  $W + 1$  jet production, where the jet is misidentified as a photon, is under control if a large photon transverse momentum cut [5] is imposed. The effects of higher order QCD corrections can largely be compensated by imposing a jet veto [2]. However, due to the very large top quark production cross section at supercollider energies, the process  $pp \rightarrow t\bar{t}\gamma \rightarrow W\gamma + X$  represents a potentially dangerous background.

Here we report on a calculation of the  $t\bar{t}\gamma$  background to  $W\gamma + X$  production at the SSC. Our calculation fully incorporates the subsequent decay of the top quarks

---

\*To appear in the Proceedings of the Workshop “Physics at Current Accelerators and the Supercollider”, Argonne National Laboratory, June 2 – 5, 1993.

into a  $W$  boson and a  $b$ -quark, and also the  $W$  decay into a fermion antifermion pair. Besides the lowest order contributions to the associated production of a  $t\bar{t}$  pair and a photon, we also include photon bremsstrahlung in  $t\bar{t}j$  events in our calculation, using the photon fragmentation approach. If no cuts are imposed on the hadrons in  $pp \rightarrow t\bar{t}\gamma \rightarrow W\gamma + X$ , the  $t\bar{t}\gamma$  production rate is found to be approximately a factor 10 (2) larger than the lowest order  $W\gamma$  cross section for a top quark mass of  $m_t = 110$  GeV (200 GeV). This considerably reduces the sensitivity of the inclusive process  $pp \rightarrow W\gamma + X$  to anomalous  $WW\gamma$  couplings. However, the  $t\bar{t}\gamma$  background can easily be reduced to a manageable level by requiring the photon to be isolated from the hadrons in the event, and by imposing a jet veto, *i.e.* by considering the exclusive reaction  $pp \rightarrow W\gamma + 0 \text{ jet}$ .

## 2. The Inclusive $t\bar{t}\gamma$ Cross Section

In our calculation of the  $pp \rightarrow t\bar{t}\gamma$  cross section we take into account the full set of lowest order  $q\bar{q} \rightarrow t\bar{t}\gamma \rightarrow W^+W^-b\bar{b}\gamma \rightarrow f_1\bar{f}_2f_3\bar{f}_4b\bar{b}\gamma$  and  $gg \rightarrow t\bar{t}\gamma \rightarrow W^+W^-b\bar{b}\gamma \rightarrow f_1\bar{f}_2f_3\bar{f}_4b\bar{b}\gamma$  Feynman diagrams. Graphs where the photon is radiated from one of the  $t$  or  $\bar{t}$  decay products are not included. The contribution from these diagrams is strongly suppressed if a photon  $p_T$  cut of  $p_T(\gamma) > m_t/2$  is imposed. The top quark and  $W$  boson decays are treated in the narrow width approximation in our calculation. Our results for  $pp \rightarrow t\bar{t}\gamma$  agree well with those presented in Ref. [6].

The bremsstrahlung contribution is calculated using the QCD  $q\bar{q} \rightarrow t\bar{t}g$ ,  $qg \rightarrow t\bar{t}q$  and  $gg \rightarrow t\bar{t}g$  matrix elements together with the leading-logarithm parametrization of Ref. [7] for the photon fragmentation functions

$$zD_{\gamma/q}(z, Q^2) = F \left[ \frac{Q_q^2(2.21 - 1.28z + 1.29z^2)z^{0.049}}{1 - 1.63\ln(1-z)} + 0.0020(1-z)^{2.0}z^{-1.54} \right], \quad (1)$$

$$zD_{\gamma/g}(z, Q^2) = \frac{0.194}{8} F (1-z)^{1.03} z^{-0.97}, \quad (2)$$

where  $Q_q$  is the electric charge of the quark  $q$  (in units of the proton charge  $e$ ),  $F = (\alpha/2\pi) \ln(Q^2/\Lambda_{QCD}^2)$ , and  $z$  is the momentum fraction of the quark or gluon carried by the photon. Since  $\alpha_s(Q^2) = 12\pi/[(33 - 2N_F) \ln(Q^2/\Lambda_{QCD}^2)]$ , these fragmentation functions are proportional to  $\alpha/\alpha_s$ , and the photon bremsstrahlung contribution formally is of the same order in  $\alpha$  as the lowest order  $t\bar{t}\gamma$  cross section.

In our subsequent analysis we focus completely on  $pp \rightarrow W^+\gamma + X$ . The cross sections of the  $t\bar{t}\gamma$  background are equal for the  $W^+\gamma + X$  and  $W^-\gamma + X$  channel. The  $pp \rightarrow W^-\gamma + X$  signal rate is approximately 20% smaller than the  $pp \rightarrow W^+\gamma + X$  cross section for the cuts specified below. Our conclusions therefore directly apply also to the  $W^-\gamma$  case.

The  $W^+$  boson is assumed to decay into a  $\ell^+\nu$  final state with  $\ell = e, \mu$ . In order to simulate the finite acceptance of detectors and to reduce fake backgrounds from jets misidentified as photons and particles lost in the beam pipe [5], we impose

the following transverse momentum, pseudorapidity and separation cuts:

$$p_T(\ell^+) > 25 \text{ GeV}, \quad |\eta(\ell^+)| < 3.0, \quad (3)$$

$$p_T(\gamma) > 100 \text{ GeV}, \quad |\eta(\gamma)| < 2.5, \quad (4)$$

$$\not{p}_T > 50 \text{ GeV}, \quad \Delta R(\ell^+, \gamma) > 0.7. \quad (5)$$

No cuts are imposed on the  $b$ -quark jets and the decay products of the second  $W$  (*i.e.* the  $W^-$ ) in  $t\bar{t}\gamma$  events.  $W^- \rightarrow \tau\nu_\tau$  decays are, for simplicity, treated like  $W^- \rightarrow e\nu, \mu\nu$ . This ignores the contribution of the one or two additional neutrinos in  $W \rightarrow \tau\nu$  to the  $\not{p}_T$  vector. Since the  $\tau$  decay channel of the  $W^-$  contributes only about 11% to the total  $W$  decay rate, the error introduced by ignoring the subsequent  $\tau$  decay is at best of the order of a few per cent, and thus much smaller than other uncertainties in the calculation, *e.g.* those originating from the choice of the factorization scale  $Q^2$ . For the parton distribution functions we use the HMRSB set [8], evaluated at  $Q^2 = \hat{s}/4$ , where  $\hat{s}$  is the parton center of mass energy squared.

Figure 1 shows the  $p_T(\gamma)$  distribution for  $pp \rightarrow t\bar{t}\gamma + X \rightarrow \ell^+ \not{p}_T \gamma + X$  at the SSC for  $m_t = 110 \text{ GeV}$  (solid line), which approximately corresponds to the present lower top quark mass limit [9], and  $m_t = 200 \text{ GeV}$  (dashed line), which is at the upper end of the range currently believed to be consistent with the SM [10]. The photon bremsstrahlung cross section is approximately 40 – 65% of the lowest order  $pp \rightarrow t\bar{t}\gamma$  rate over the entire  $p_T(\gamma)$  range shown in Fig. 1. The shape of the photon transverse momentum distribution depends on the top quark mass, with the  $p_T(\gamma)$  distribution becoming harder for increasing values of  $m_t$ .

The dotted curve in Fig. 1 shows the lowest order prediction of the photon transverse momentum distribution for the  $W^+\gamma$  signal. The  $t\bar{t}\gamma$  background is seen to be much larger than the cross section of the signal over the entire top quark mass range studied. For a heavy top quark, the background is largest at high photon transverse momenta which is exactly the region where non-standard  $WW\gamma$  couplings result in large deviations from the SM [3]. It is obvious from Fig. 1 that the  $t\bar{t}\gamma$  background will considerably reduce the sensitivity of  $pp \rightarrow W^+\gamma + X$  to non-standard  $WW\gamma$  couplings.

### 3. Jet Veto

Since the top quark decays predominantly into a  $Wb$  final state,  $t\bar{t}\gamma$  events are characterized by a large hadronic activity which frequently results in one or several high  $p_T$  jets. If the second  $W$  boson decays hadronically, up to four jets are possible. This observation suggests that the  $t\bar{t}\gamma$  background may be suppressed by vetoing high  $p_T$  jets. Such a “zero jet” requirement has been demonstrated [2] to be very useful in reducing the size of NLO QCD corrections in  $pp \rightarrow W\gamma + X$  at SSC energies. Present studies [5, 11] suggest that jets with  $p_T > 50 \text{ GeV}$  can be identified at the SSC without problems, whereas it will be difficult to reconstruct a jet with a transverse momentum smaller than about 30 GeV. In the following we

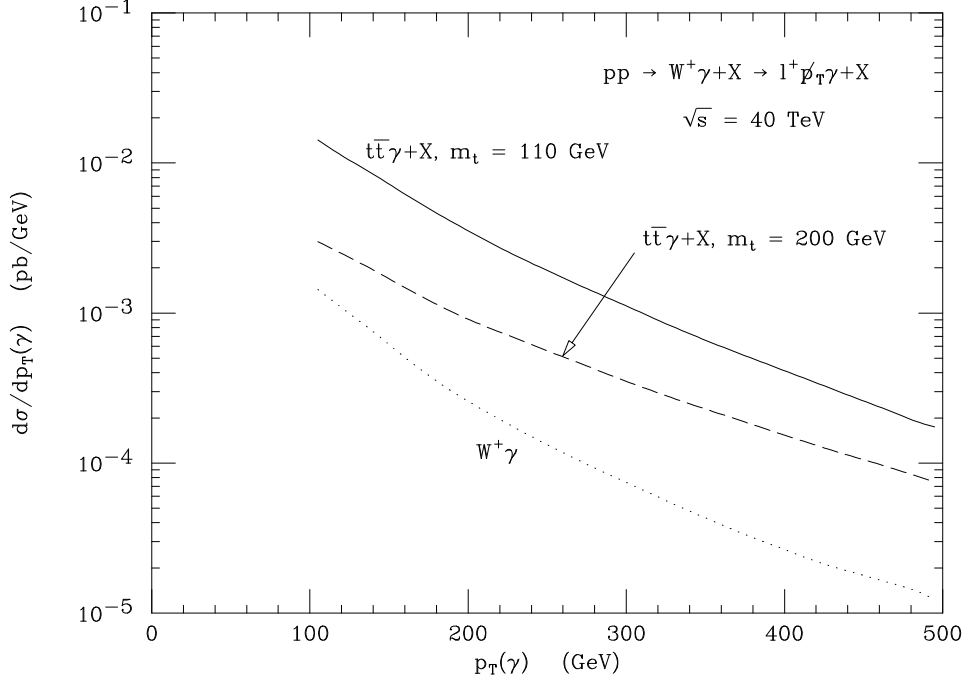


Figure 1: The photon transverse momentum distribution for  $pp \rightarrow W^+\gamma + X \rightarrow \ell^+p_T\gamma + X$  at the SSC. The solid (dashed) line shows the result for  $t\bar{t}\gamma + X$  production for  $m_t = 110$  GeV (200 GeV). The dotted line gives the tree level SM prediction of the  $W^+\gamma$  signal. The cuts imposed are summarized in Eqs. (3) – (5).

therefore require that

$$\text{no jets with } p_T(j) > 50 \text{ GeV} \quad \text{and} \quad |\eta(j)| < 3 \quad (6)$$

are observed in  $W\gamma$  events. In order to further suppress the  $t\bar{t}\gamma$  background, we also require the photon to be isolated from the hadronic activity [11]:

$$\sum_{\Delta R < 0.4} E_{\text{had}} < 4 \text{ GeV}, \quad (7)$$

with  $\Delta R = [(\Delta\phi)^2 + (\Delta\eta)^2]^{1/2}$ . The photon isolation cut is especially useful in suppressing the photon bremsstrahlung contribution.

If the second  $W$  in  $t\bar{t}\gamma$  events decays hadronically, the number of jets in  $pp \rightarrow t\bar{t}\gamma \rightarrow W^+\gamma + X$  is in general larger than for leptonic  $W$  decays, and the jet veto is more efficient. In order to reduce the  $t\bar{t}\gamma$  background for leptonic decays of the second  $W$  sufficiently, we also impose a veto on a second charged lepton in the pseudorapidity region  $|\eta| < 3$ . For leptons with a sufficiently large transverse momentum,  $p_T(\ell) > 15$  GeV, it should be possible to implement this requirement rather easily. For small lepton transverse momenta, tracks in minimum bias events which are misidentified as electrons, and decays in flight of kaons and pions constitute a potential problem. Fortunately, most  $W$  decay leptons have a transverse

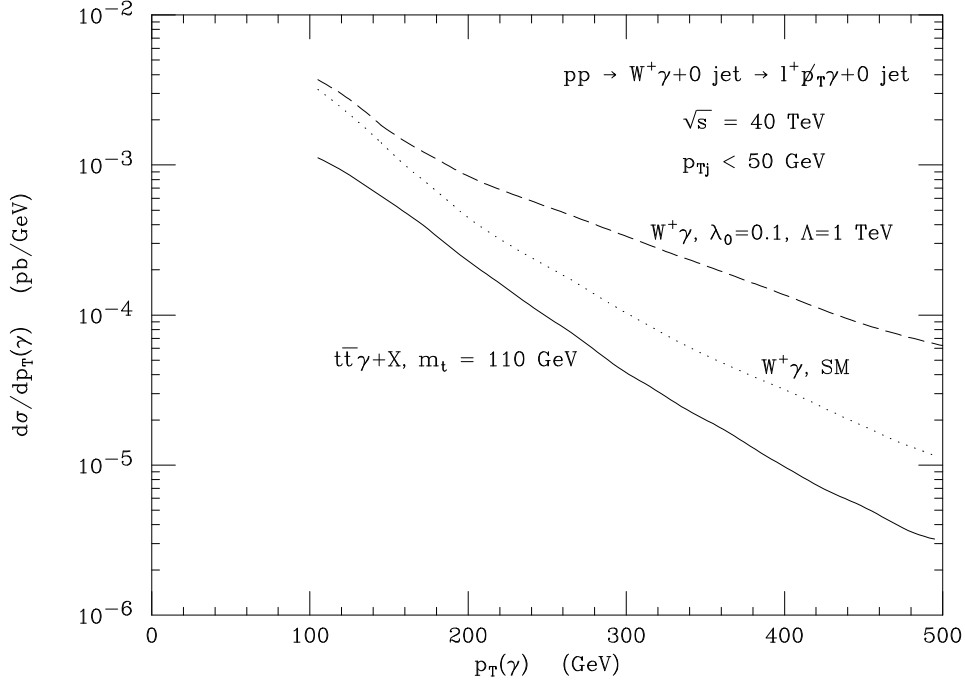


Figure 2: The photon transverse momentum distribution for  $pp \rightarrow W^+\gamma + 0 \text{ jet} \rightarrow \ell^+ \cancel{p}_T \gamma + 0 \text{ jet}$  at the SSC. The solid line shows the result for the  $t\bar{t}\gamma$  background with  $m_t = 110 \text{ GeV}$ . The dotted and dashed lines give the NLO prediction of the  $p_T(\gamma)$  distribution for the  $W^+\gamma + 0 \text{ jet}$  signal in the SM, and for a non-standard  $WW\gamma$  coupling  $\lambda_0 = 0.1$  and dipole form factor scale  $\Lambda = 1 \text{ TeV}$ , respectively. The cuts imposed are described in the text.

momentum larger than 15 GeV. Our results change by about 15% if the charged lepton veto is only implemented in the region  $p_T > 15 \text{ GeV}$ . For  $|\eta| > 3$ , we assume that leptons are not detected and contribute to the missing transverse momentum in the event.

Figure 2 shows the photon  $p_T$  distribution for  $pp \rightarrow t\bar{t}\gamma + X \rightarrow W^+\gamma + 0 \text{ jet}$  with  $m_t = 110 \text{ GeV}$  and the jet and lepton veto cuts described above (solid line). The result is compared with the NLO QCD  $pp \rightarrow W^+\gamma + 0 \text{ jet}$  result in the SM (dotted curve), and for a non-standard  $WW\gamma$  coupling (dashed line)

$$\lambda = \frac{\lambda_0}{(1 + m_{W\gamma}^2/\Lambda^2)^2}, \quad (8)$$

with  $\lambda_0 = 0.1$  and form factor scale  $\Lambda = 1 \text{ TeV}$ . For a definition of  $\lambda$  see *e.g.* Refs. [1, 2]. In the SM, at tree level,  $\lambda_0 = 0$ .  $m_{W\gamma}$  in Eq. (8) is the  $W\gamma$  invariant mass. The form factor nature of the anomalous coupling is introduced to avoid violation of  $S$ -matrix unitarity [3]. The  $\mathcal{O}(\alpha_s)$   $pp \rightarrow W^+\gamma + 0 \text{ jet}$  cross section has been obtained using the results of Ref. [2]. NLO QCD corrections are quite significant at low photon transverse momenta for  $W\gamma$  production at the SSC, even

Table 1: Contributions to the total  $pp \rightarrow t\bar{t}\gamma \rightarrow \ell^+ \cancel{p}_T \gamma + 0$  jet cross section at the SSC for two jet defining  $p_T$  thresholds. All other cuts are specified in the text. For comparison, the last line gives the inclusive  $pp \rightarrow t\bar{t}\gamma + X \rightarrow \ell^+ \cancel{p}_T \gamma + X$  cross section, imposing only the cuts listed in Eqs. (3) – (5).

| channel                                   | $p_T(j)$ (GeV) | cross section (pb)  |                     |
|---|----------------|---------------------|---------------------|
|   |                | $m_t = 110$ GeV     | $m_t = 200$ GeV     |
| direct, $W^- \rightarrow jj$              | $< 50$         | 0.051               | $7.9 \cdot 10^{-4}$ |
|   | $< 35$         | 0.014               | $1.9 \cdot 10^{-4}$ |
| direct, $W^- \rightarrow \ell\nu$         | $< 50$         | 0.014               | $3.5 \cdot 10^{-4}$ |
|   | $< 35$         | 0.010               | $1.8 \cdot 10^{-4}$ |
| $\gamma$ brem., $W^- \rightarrow jj$      | $< 50$         | $7.7 \cdot 10^{-3}$ | $1.0 \cdot 10^{-4}$ |
|   | $< 35$         | $1.9 \cdot 10^{-3}$ | $3.4 \cdot 10^{-5}$ |
| $\gamma$ brem., $W^- \rightarrow \ell\nu$ | $< 50$         | $2.1 \cdot 10^{-3}$ | $5.6 \cdot 10^{-5}$ |
|   | $< 35$         | $1.4 \cdot 10^{-3}$ | $3.2 \cdot 10^{-5}$ |
| total                                     | $< 50$         | 0.075               | $1.3 \cdot 10^{-3}$ |
|   | $< 35$         | 0.027               | $4.4 \cdot 10^{-4}$ |
| total, no jet veto                        | –              | 1.09                | 0.27                |

if a zero jet cut is imposed. We have therefore opted to compare the  $t\bar{t}\gamma$  background with the  $\mathcal{O}(\alpha_s)$  prediction for the signal instead of the tree level result.

Figure 2 demonstrates that vetoing jets with  $p_T(j) > 50$  GeV reduces the  $t\bar{t}\gamma$  cross section sufficiently so that the sensitivity to anomalous  $WW\gamma$  couplings is not significantly affected. At low (high) transverse momentum, the cuts of Eqs. (6) and (7) suppress the  $t\bar{t}\gamma$  rate by about a factor 15 (70).

Details of the various contributions to the total  $pp \rightarrow t\bar{t}\gamma \rightarrow W^+\gamma + 0$  jet rate at the SSC for  $m_t = 110$  GeV and  $m_t = 200$  GeV are shown in Table 1. Due to the photon isolation requirement, the contribution of photon bremsstrahlung is reduced to  $\sim 15\%$  of the direct  $t\bar{t}\gamma$  cross section. The veto on a second charged lepton in the event significantly suppresses the channel where the second  $W$  decays leptonically.

With increasing top quark mass, the  $p_T$  distribution of the  $b$ -quark jets, and the jets from  $W$  decay, becomes harder. The jet veto cut, therefore, is more efficient at large values of  $m_t$ . For  $m_t = 200$  GeV the  $t\bar{t}\gamma + X$  cross section is reduced by about a factor 200, whereas the rate only drops by a factor 15 for  $m_t = 110$  GeV (see Table 1).

Due to the relatively large number of jets possible in  $t\bar{t}\gamma$  events, the  $pp \rightarrow t\bar{t}\gamma \rightarrow W^+\gamma + 0$  jet rate depends quite sensitively on the jet defining  $p_T$  threshold. This is detailed in Table 1, where we also list the cross sections if the jet transverse momentum threshold is lowered to 35 GeV, with all other cuts unchanged. For a jet  $p_T$  threshold smaller than about 35 GeV, SSC detectors face increasing difficulties

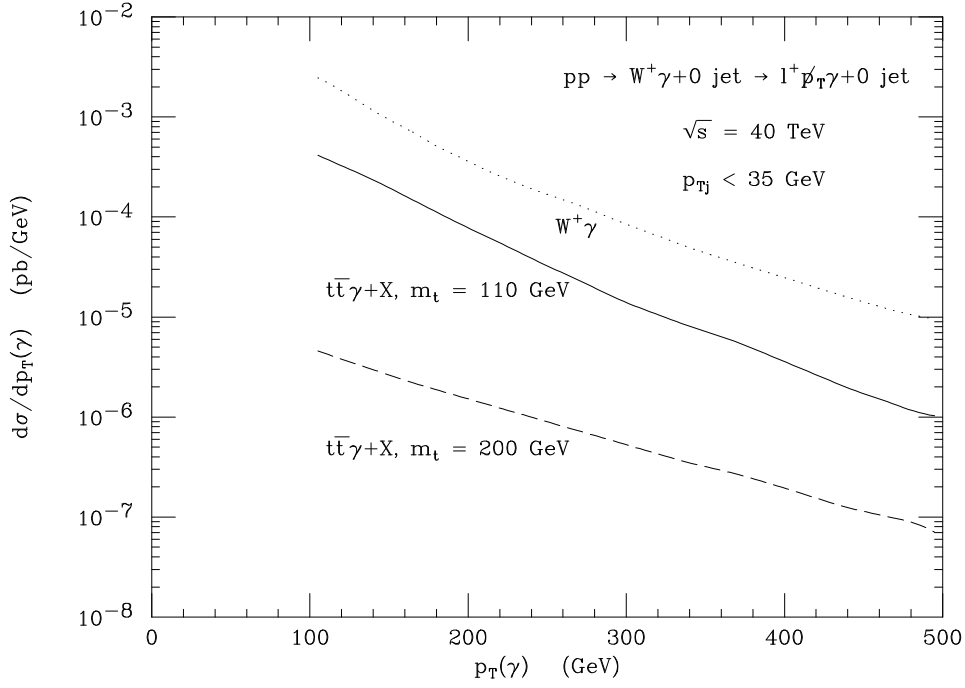


Figure 3: The photon transverse momentum distribution for  $pp \rightarrow W^+\gamma + 0 \text{ jet} \rightarrow \ell^+ p_T\gamma + 0 \text{ jet}$  at the SSC with a jet transverse momentum threshold of 35 GeV. The solid (dashed) line shows the result for the  $t\bar{t}\gamma$  background for  $m_t = 110$  GeV (200 GeV). The dotted line gives the NLO prediction of the  $p_T(\gamma)$  distribution for the  $W^+\gamma + 0 \text{ jet}$  signal in the SM.

in reconstructing jets [5, 11]. Compared to a  $p_T(j)$  threshold of 50 GeV, the  $pp \rightarrow t\bar{t}\gamma \rightarrow W^+\gamma + 0 \text{ jet}$  cross section is reduced by more than a factor 3 if the second  $W$  decays hadronically. On the other hand, for leptonic decays of the  $W^-$ , the rate drops only by about a factor 1.4 to 1.8. Overall, the  $t\bar{t}\gamma$  background can be reduced by an additional factor 3, if a jet defining  $p_T$  threshold of 35 GeV instead of 50 GeV can be employed. The  $\mathcal{O}(\alpha_s)$   $W\gamma + 0 \text{ jet}$  signal cross section drops only by approximately 20% if the jet transverse momentum threshold is lowered [2].

The photon transverse momentum distribution of the  $t\bar{t}\gamma$  background and the  $pp \rightarrow W^+\gamma + 0 \text{ jet}$  signal, calculated to  $\mathcal{O}(\alpha_s)$ , for a jet  $p_T$  threshold of 35 GeV is shown in Fig. 3. The  $t\bar{t}\gamma$  background is seen to be about one order of magnitude below the signal (dotted line) for  $m_t = 110$  GeV (solid line), and approximately two orders of magnitude for  $m_t = 200$  GeV (dashed line).

#### 4. Conclusions

We have presented a calculation of  $t\bar{t}\gamma$  production at the SSC. Our calculation takes into account the subsequent  $t \rightarrow Wb$  and  $W$  decay, and incorporates the contribution originating from photon bremsstrahlung in  $t\bar{t}j$  events. Imposing typical photon and lepton identification requirements, we found that the  $t\bar{t}\gamma$  cross section

is up to one order of magnitude larger than the tree level  $W\gamma$  rate.  $t\bar{t}\gamma$  production therefore constitutes a dangerous background to inclusive  $W\gamma$  production,  $pp \rightarrow W\gamma + X$ , which significantly reduces the sensitivity of this process to anomalous  $WW\gamma$  couplings.

In general, the  $W\gamma$  system originating from  $t\bar{t}\gamma$  events is accompanied by one or several jets. Vetoing all jets with  $p_T(j) > 50$  GeV and a second charged lepton in the pseudorapidity region  $|\eta(j)| < 3$ , the  $t\bar{t}\gamma$  background can be suppressed to a level well below the  $W\gamma + 0$  jet signal. If the jet defining transverse momentum threshold can be reduced to 35 GeV, the  $t\bar{t}\gamma$  background cross section is at most 10% of the  $W\gamma$  signal rate.

## 5. Acknowledgements

We would like to thank S. Errede and S. Keller for stimulating discussions. This research was supported in part by the U. S. Department of Energy under Contract No. DE-FG05-87ER40319, and Contract No. DE-AC02-76CH00016.

## 6. References

- [1] K. Hagiwara *et al.*, *Nucl. Phys.* **B282** (1987) 253; U. Baur and D. Zeppenfeld, *Nucl. Phys.* **B325** (1989) 253; K. Hagiwara, J. Woodside, and D. Zeppenfeld, *Phys. Rev.* **D41** (1990) 2113.
- [2] U. Baur, T. Han and J. Ohnemus, FSU-HEP-930519, to appear in *Phys. Rev.* **D**.
- [3] U. Baur and D. Zeppenfeld, *Nucl. Phys.* **B308** (1988) 127.
- [4] S. Willenbrock and D. Zeppenfeld, *Phys. Rev.* **D37** (1988) 1775.
- [5] R. Zhu, CALT-68-1777 preprint (March 1992); E. L. Berger *et al.*, SDC Technical Design Report, SDC-92-201 (April 1992).
- [6] E. Maina and S. Moretti, *Phys. Lett.* **B286** (1992) 370.
- [7] D. W. Duke and J. F. Owens *Phys. Rev.* **D26** (1982) 1600.
- [8] P. N. Harriman, A. D. Martin, R. G. Roberts, and W. J. Stirling, *Phys. Rev.* **D42** (1990) 798.
- [9] T. Liss (CDF Collaboration), talk given at the *1993 APS Meeting*, Washington, D.C., April 1993.
- [10] D. Schaile, *Z. Phys.* **C54** (1992) 387.
- [11] W. C. Lefmann *et al.* (GEM Collaboration), GEM Technical Design Report, GEM-TN-93-262 (April 1993).